Comparison of the standards of air kerma and absorbed dose to water in Co-60 radiation for the National Research Council of Canada and the Laboratorio de Metrologia de Radiaciones Ionizantes, Comisión Chilena de Energía Nuclear

McEwen, Malcolm; Rodriguez, Hernán; Ortega, Fernando; Oyarzun, Carlos

https://doi.org/10.4224/23002717

Comparison of the standards of air kerma and absorbed dose to water in Co-60 radiation for the National Research Council Canada and the Laboratorio de Metrologia de Radiaciones Ionizantes, Comisión Chilena de Energía Nuclear.

NRC·CNRC Measurement Science and Standards

Malcolm McEwen[1], Hernán Rodriguez[2], Fernando Ortega[2] and Carlos Oyarzun[2]

[1] Ionizing Radiation Standards, NRC

[2] Laboratorio de Metrologia de Radiaciones Ionizantes, CCHEN

Report PIRS-2370 March 2017

The provision of this report and results, or the use of any particular equipment described herein does not represent an endorsement by the National Research Council of such equipment for the measurement of ionizing radiation.

National Research Council Canada Conseil national de recherches Canada

Canada

Comparison of the standards of air kerma and absorbed dose to water in Co-60 radiation for the National Research Council Canada and the Laboratorio de Metrologia de Radiaciones Ionizantes, Comisión Chilena de Energía Nuclear.

Report PIRS-2370

Malcolm McEwen, Hernán Rodriguez, Fernando Ortega and Carlos Oyarzun

Abstract

An indirect comparison has been made of the standards for air kerma and absorbed dose to water in ^{60}Co radiation of the National Research Council (NRC), Canada and of the Laboratorio de Metrologia de Radiaciones Ionizantes (LMRI), Chile. The measurements at the LMRI were carried out in October 2016. The comparison results, based on the calibration coefficients for one transfer standard and evaluated as a ratio of the LMRI and the NRC standards, were 0.9972 for absorbed dose to water, with a combined standard uncertainty of 8.9×10^{-3}, and 0.9945 for air kerma, with a combined standard uncertainty of 8.6×10^{-3}. The results are analysed in the context of the degrees of equivalence for these quantities published in the BIPM key comparison database. Additional characterization of the LRMI Co-60 irradiator is also described.

1. Introduction

A new suite of laboratory facilities is being constructed at the Comisión Chilena de Energía Nuclear (CCHEN) to provide expanded capabilities for the Laboratorio de Metrologia de Radiaciones Ionizantes (LMRI). One of the major additions is a therapy-level Co-60 facility that will provide calibration services and reference irradiations for Chilean cancer centres. Soon after the installation of the irradiator, a comparison was arranged with the National Research Council Canada (NRC) to confirm the LMRI dissemination of air kerma and absorbed dose to water.

2. Commissioning of Theratron Co-60 source at LMRI

The Theratron Co-60 irradiator installed at LMRI is very similar in design to the Gammabeam X-200 Co-60 irradiator used at NRC. Although in a comparison of reference chambers there should be no significant dependence on the Co-60 field, the similarity of the irradiators reduces the possibility of any difference in the comparison being due to the radiation field. Figure 1 shows the calibration setups at the two facilities. The major difference is that the trimmer bars are not installed on the NRC unit, which results in a broader penumbra for the NRC field compared to the LMRI field.

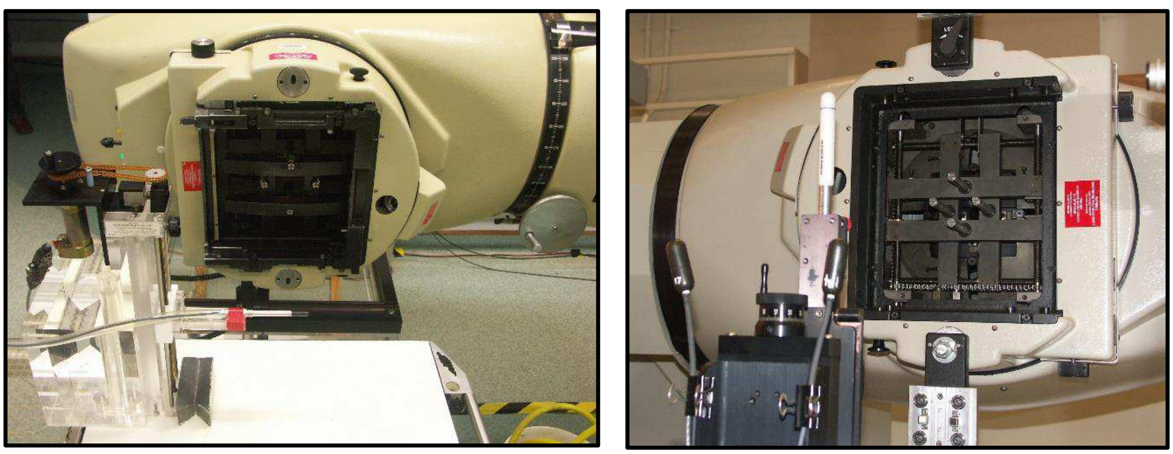

Figure 1. In-air measurement set-ups for LMRI (left) and NRC (right). The major difference is that the trimmer bars are not installed on the NRC unit (see the four rods near the centre).

During the commissioning of the LMRI irradiator, a number of performance characteristics were studied, including shutter timing error; radial profiles, output factors, and depth-dose curves.

2.1 Shutter timing error

Measurements were made to verify that the irradiation beam-time indicated by the control unit was accurate. An ion chamber was placed in the centre of the radiation field (similar to the set up in Figure 1a above) and a series of timed irradiations was delivered. If there is no shutter timing error then the mean ionization current will be independent of the indicated irradiation time. The results are shown in Table 1.

Table 1. Measurement of shutter error

t_{set} (s)	R (nC)	I (pA)
15	1.443	96.20
30	2.892	96.40
45	4.341	96.47
60	5.788	96.47
90	8.685	96.50
120	11.58	96.50

The data shows a slight dependency of the ionization current on the set irradiation time, indicating a slight offset between the set time and the actual irradiation. A linear fit of the chamber reading, R, versus t_{set} yields a timer correction of -46 ms (i.e., the actual irradiation time is less than the set time). This value is consistent with that of the NRC Co-60 unit and, as can be seen in the table, any effect is only significant for short irradiation times of 30 s or less.

2.2 Beam profiles

Radial beam profiles were acquired in both air and water for the LMRI unit. The in-air measurements were acquired as shown in Figure 1a, using the CNMC water phantom 1-D axis system, removed from the water phantom. The chamber Co-60 build-up cap was fitted after setting the correct SCD. The results are shown in Figure 2.

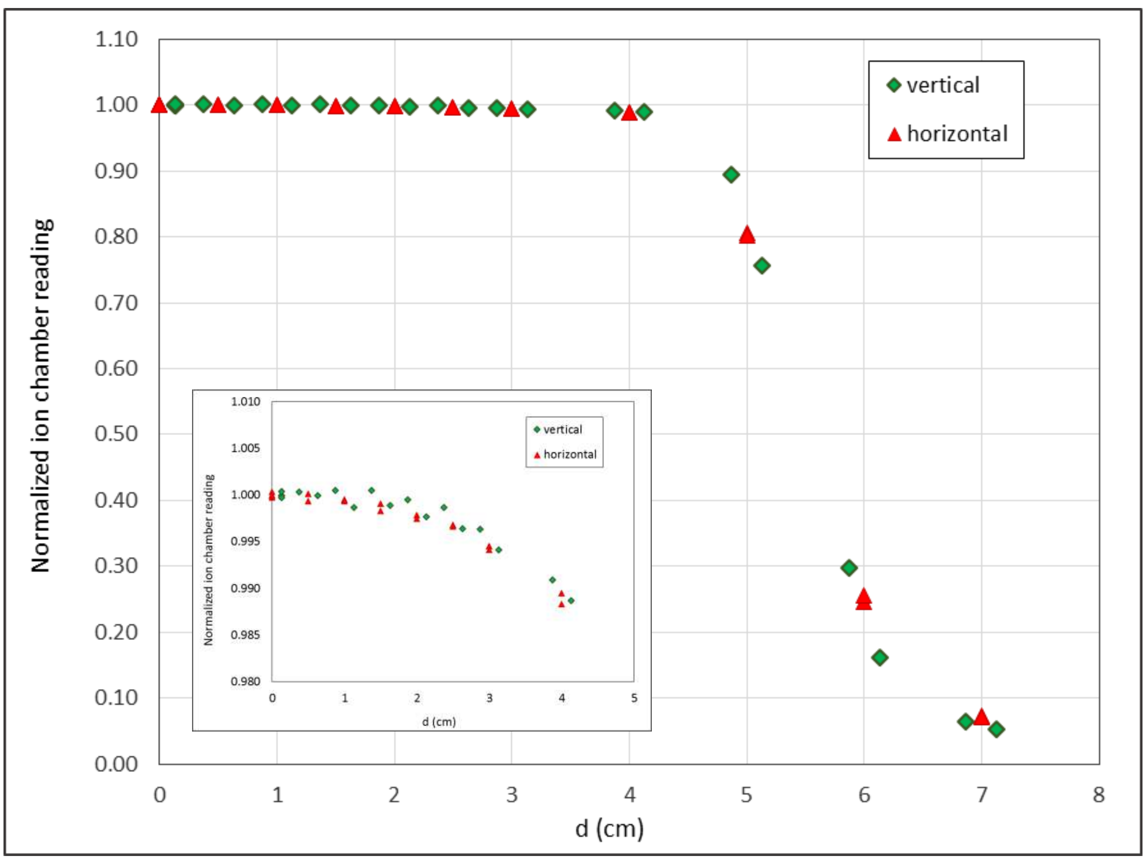

Figure 2. In-air beam profiles (vertical and horizontal) for a nominal 10 cm x 10 cm field size and measured SCD = 80 cm. The data has been mirrored about the central axis to show symmetry and flatness.

The inset plot in Figure 2 is a blow-up of the central 8 cm of the field (which appears completely flat in the main plot. The apparent noise in the vertical plot is the due to the interleaving of the data above and below the centre position. There is a slight asymmetry and when the data for negative positions is mirrored the result is the “zig-zag” distribution. The actual level of noise can be estimated from the horizontal plot, yielding a value of 0.2 %. The variation in beam flatness for the dimensions of the chambers used in the comparison is 0.1 %.

For the water profiles, the same 1-D axis system was placed in the filled water phantom, as shown in Figure 3a. Only a vertical scan was possible but it was assumed that the symmetry between vertical and horizontal profiles was similar to that of the in-air measurements. The results are shown in Figure 3b.

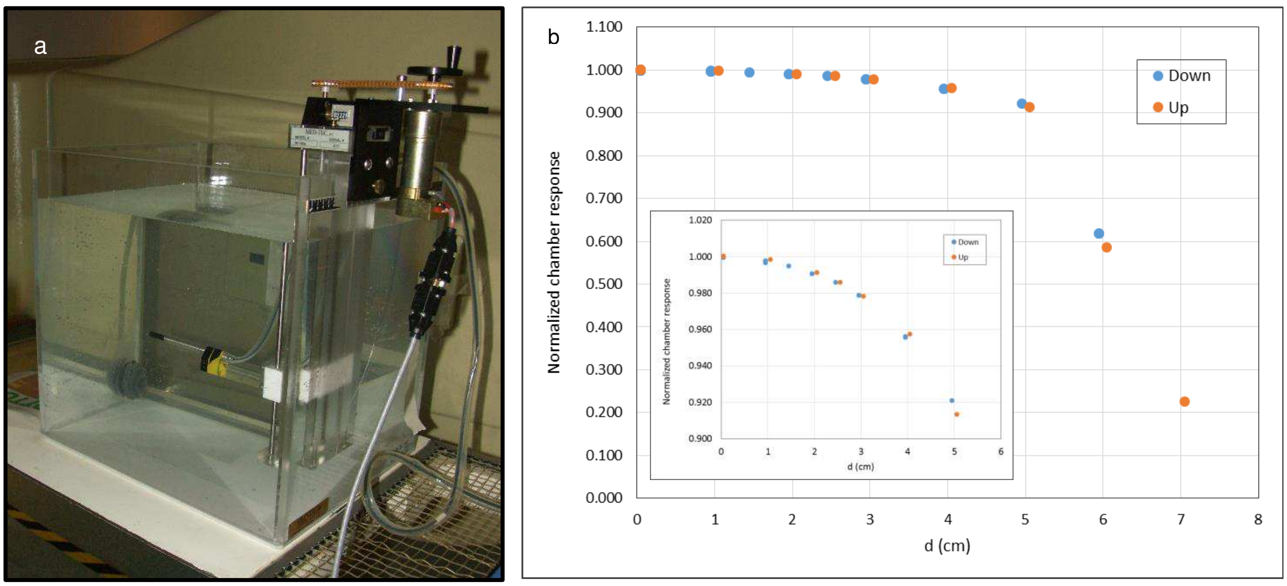

Figure 3. Experimental setup (a) and results for measurements of in-water dose profile (b).

As expected from other calibration laboratories, the flatness is superior for the in-air situation, compared to in-water. However, even for the water situation the volume averaging effect for a Farmer-type ionization chamber (thimble length ~ 25 mm) is only around 0.15 %. For a shorter thimble chamber, such as the NE2611 the correction for volume averaging is of the order of 0.05 %.

2.3 Output factors

Output factors were measured by varying the field size for an ionization chamber positioned at the field centre. The results are shown in Figure 4. The sensitivity of the chamber reading for the 10 cm x 10 cm field is ~ 2.7 % per cm (for a change in both axes), so care is required to ensure that the correct field size is set. Mechanical verification of the actual collimator setting is recommended, to avoid read-out errors of the field-size scales, or hysteresis in the adjustment mechanism.

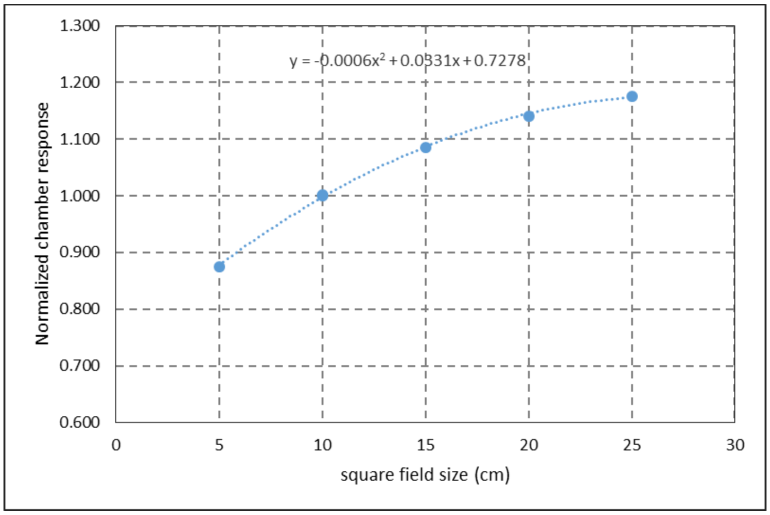

Figure 4. Variation in chamber response as a function of field size. The chamber was positioned in the centre of the field using the light field and the field size was read-off from the "55" line on the field-adjustment scales.

2.4 Depth-dose

A depth-ionization curve was acquired using the IBA FC65-G ionization chamber with the beam positioned vertically. The ionization chamber was scanned in one direction, as recommended by the AAPM TG-106 report, from deep in the phantom to above the water surface. The position of the water surface was determined using the reflective symmetry method described in TG-106 (Das *et al*, 2008) and verified by visually identifying the position where the out edge of the chamber thimble broke the water surface. Figure 5 shows the first of these two methods. The difference between the two measurements should equal the outer radius of the chamber and this was found to be the case within 0.2 mm.

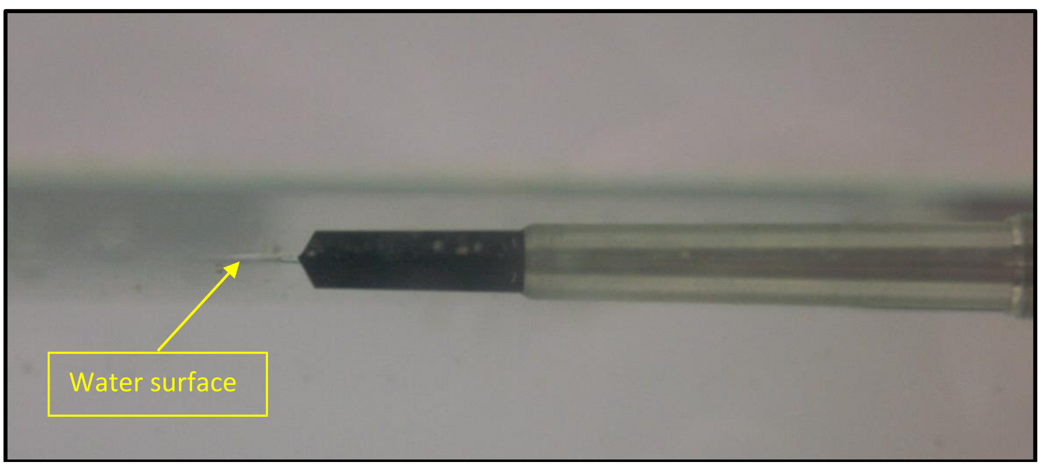

Figure 5. IBA FC65-G ionization chamber at the positioned at the water surface. The position of the surface is visible in this image due to the disturbance caused by the chamber (it is more obvious in real-life).

Figure 6 shows the experimental data, compared to that tabulated in Table 4.3 of BJR Supplement 25 (for 80 cm SSD, 10 cm x 10 cm field size). As can be seen the agreement is very good with maximum differences at the 1 % level (of the local dose reading, not the peak reading). This level of agreement is perhaps to be expected, since the LMRI Co-60 unit is a 'standard' clinical device, but it confirms that the calibration beam of the LMRI is consistent with clinical beams. The continuation of the measurement above the water surface can be used to retrospectively determine the origin for the measurement (Ververs, *et al*, 2009). The resolution of the data is more coarse than desired for this technique but it yields a value for the origin within 0.4 mm of the visual method. One issue noted during the measurements was that the chamber movement mechanism changes the water level due to volume displacement as it moves the chamber from the surface to the measurement point (e.g., 10 cm). The effect was significant, with a shift of up to 1 mm in apparent depth, and therefore a modified holder, which eliminates this change in displacement is recommended.

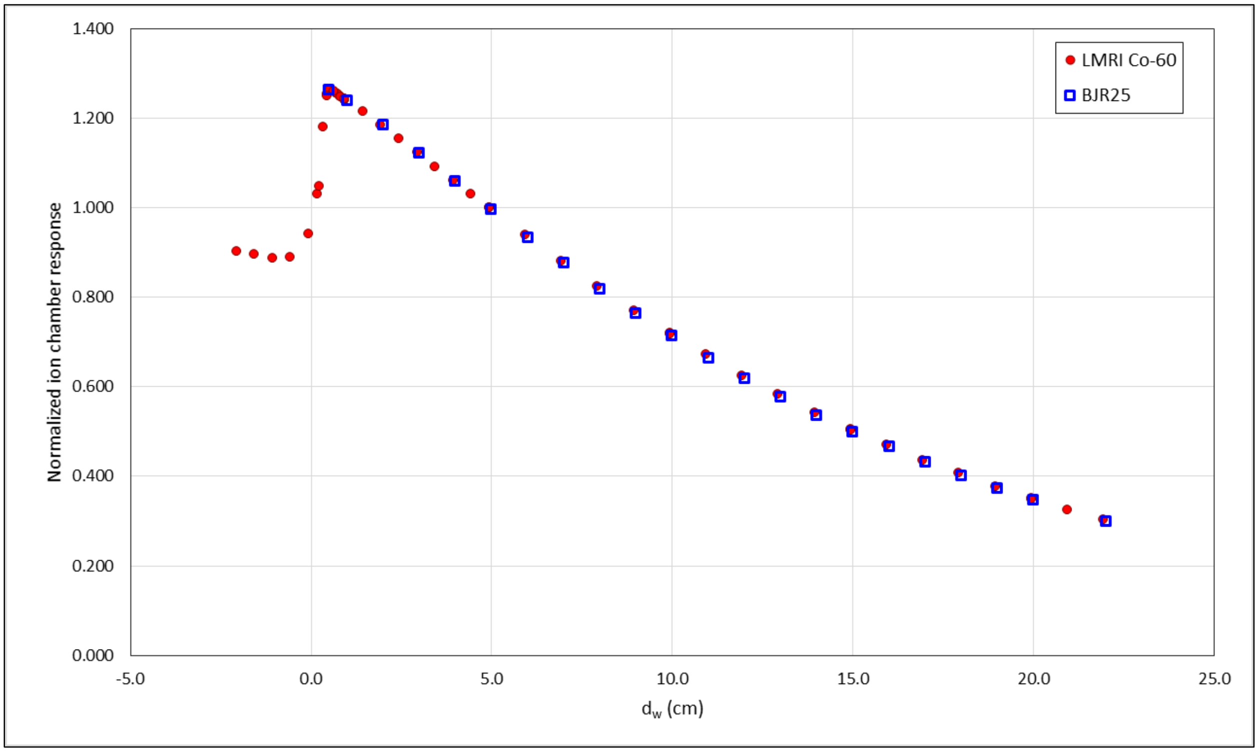

Figure 6. Depth-ionization curve, obtained for a vertical beam (i.e., no entrance window). The field size was set to 10 x 10 cm with an SSD of 80 cm. The measured data is corrected for the effective point of measurement of the IBA FC65-G ion chamber and compared with standard data from BJR Supplement 25 for the same field size and SSD.

3. Comparison measurements

3.1 NRC transfer ionization chamber

The transfer chamber for the comparison was an IBA FC65-G S/N1233, waterproof Farmer-type chamber with a graphite thimble and aluminium central electrode. The chamber has been used as a working standard at NRC since 2008 for some time and has demonstrated stability at the level required for a transfer instrument (standard deviation < 0.08% over six years).

Prior to the comparison the chamber was calibrated in terms of air kerma and absorbed dose to water in the NRC Co-60 facility. The chamber was also measured again after returning from CCHEN, but only in terms of absorbed dose to water as experience indicates a strong correlation between absorbed dose and air kerma responses. The calibration data are shown in Tables 2 & 3. Two electrometers were used for the NRC measurements – a Keithley 35617, which is the standard instrument used for all Co-60 ion chamber calibrations at NRC, and a Standard Imaging Supermax S/N P082341, which was the electrometer that was taken to LMRI. For all measurements, at least 25 minutes pre-irradiation was carried out before each measurement. A very long irradiation of 60 minutes was carried out between the first and second air kerma measurement to investigate any longer-term stabilization effect. No difference was seen at the level of the Type A uncertainties.

Table 2. Measurements of transfer chamber IBA FC65-6 S/N1233 at NRC; before comparison – air kerma

Date	Electrometer	HT[1] (V)	I_{corr}[2] (nA)	std unc (%) (Type A)
20-Sep-16	Keithley 35617	-300	0.31149	0.01
20-Sep-16	Keithley 35617	-300	0.31152	0.01
20-Sep-16	Keithley 35617	+300	-0.31136	0.01

[1] Polarizing voltage indicated is that applied to the central, collecting electrode of the ionization chamber.
[2] Air kerma rate = 0.95 Gy min^{-1}.

Table 3. Measurements of transfer chamber IBA FC65-6 S/N1233 at NRC; before and after comparison – absorbed dose to water

Date	Electrometer	HT[1] (V)	I_{corr}[2, 3] (nA)	std unc (%) (Type A)
19-Sep-16	Keithley 35617	-300	0.25477	0.01
19-Sep-16	Keithley 35617	+300	-0.25453	0.01
19-Sep-16	SI Supermax	+300	-0.25458	0.04
19-Sep-16	SI Supermax	-300	0.25480	0.03
19-Sep-16	Keithley 35617	-300	0.25476	0.01
28-Oct-16	Keithley 35617	-300	0.25464	0.01

[1] Polarizing voltage indicated is that applied to the central, collecting electrode of the ionization chamber.
[2] Corrected for source decay to reference date of 19-Sep-16 to compare "before" and "after" measurements.
[3] Absorbed doserate to water = 0.73 Gy min^{-1}.

Combining the ionization chamber readings (corrected for temperature, pressure and humidity) with the known absorbed dose to water and air kerma rates on the reference dates (19-Sep-16 and 20-Sep-16 respectively) yielded calibration coefficients for the two quantities of:

N_K (1233) = 44.69 mGy/nC

$N_{D,w}$ (1233) = 48.52 mGy/nC

3.2 LMRI reference chambers

LMRI currently obtains its traceability for Co-60 air kerma and absorbed dose to water from the National Physical Laboratory (NPL). A number of NE2561 and NE2611 chambers have been calibrated at the NPL over many years and these are shown in Table 4.

Table 4. Traceability of LMRI secondary standard ionization chambers.

Type	S/N	Calibration quantity	Calibration date
NE2561	303	Air kerma	1988
NE2611	247	Air kerma	2009
NE2611	1023	Absorbed dose to water	2015

Chamber #247 proved very unstable and therefore could not be used; Chamber #303 and #1023 both showed reference chamber stability and repeatability. However, the validity of applying the 1988 calibration without interim stability measurements means that chamber #1023 is the primary reference for the comparison. Although an air kerma calibration coefficient was not included in the 2015 calibration, a derived calibration was obtained by applying a generic C_K value (ratio of air kerma to absorbed dose). The C_K value was obtained from anonymous NE2611 calibration data provided by NPL (Nutbrown, 2013): C_K ($_{D,w}/N_K$) = 1.0797. The standard deviation on the distribution of values was 0.13 %, which is taken to be the standard uncertainty in applying this generic value to chamber #1023. The calibration coefficients for the LMRI standard are therefore:

N_K (1023) = 94.1 mGy/nC

$N_{D,w}$ (1023) = 101.5 mGy/nC

The resolution of these coefficients is as provided on the NPL calibration certificate.

3.3 Environmental conditions

The corrections for temperature and pressure have a direct impact on the ionization chambers measurements required for the comparison. The respective environmental conditions in the two laboratories are given in Table 5.

Table 5. Environmental conditions in NRC and LMRI laboratories during comparison period

Location	P (kPa)	T_{air} (°C)	T_{water} (°C)	RH (%)
NRC	100.6	21.9	21.9	40
LMRI	93.2	19.7	19.2	N/A

Temperature control in both laboratories was very good, with stability at better than ± 0.2 °C. Pressure variations were small within the course of any one day (typically less than 0.2 kPa) and also small from day-to-day (less than 0.5 kPa). However, there is a significant difference in the absolute air pressure values due to the altitudes of Ottawa (close to sea level) and Santiago (~ 500 m). Humidity was around RH = 40 % at NRC. It was not monitored at the LMRI but the temperature differential between water and air measurements suggests that the relative humidity was less than at NRC. No effect of humidity on the ion chambers used in this comparison is anticipated.

3.4 Stabilization of ionization chambers

It has been shown (e.g., McCaffrey *et al*, 2005; McEwen, 2010) that ionization chambers in Co-60 beams can require a significant pre-irradiation to reach a stable reading. Similar to the procedure noted above for the NRC measurements, each chamber in the LMRI beam was pre-irradiated for at least 20 minutes and the chamber reading was monitored during this time. The results are shown in Figure 7.

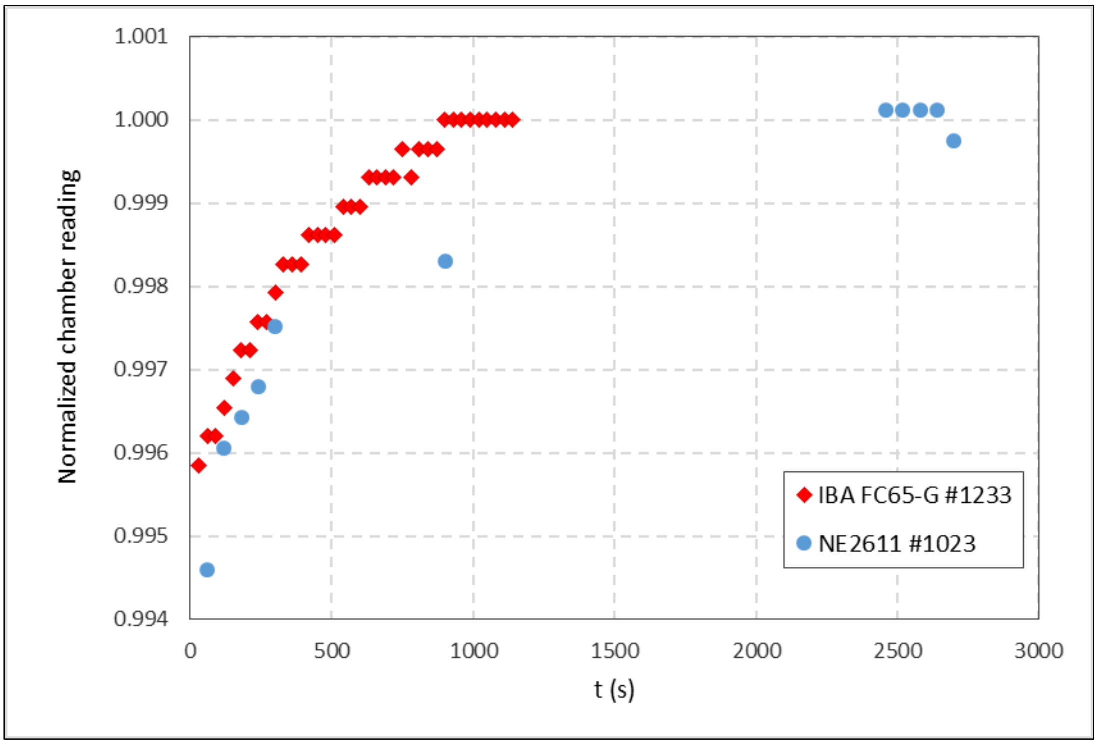

Figure 7. Response of NRC and LMRI reference chambers in LMRI Co-60 beam (air kerma measurement). The procedure followed was that the polarizing voltage was applied, the beam was switched on and then data collection commenced. The stabilization behavior (initial offset and equilibration time) is consistent with that reported in the literature. The apparent step in the ionization current at the end of the plot for chamber #1023 indicates the resolution of the electrometer.

The longer equilibration time seen for the NE2611 chamber is to be expected as it had not been irradiated for some time. Figure 7 shows the initial response to radiation. Irradiations on subsequent days resulted in stabilization at the ± 0.03 % level within five minutes.

3.5 Polarity and recombination corrections

In ion chamber comparisons in a Co-60 beam it is often the case that no polarity correction is applied as it is assumed that there is no difference in the polarity response of the chamber between the two irradiation fields. For this comparison the polarity correction for chamber #1233 was measured as an additional QA metric, to ensure correct operation of the transfer chamber in the LMRI beam. The results are shown in Table 6. There is very good agreement between in-water and in-air measurements, and no dependence on electrometer type or the particular Co-60 beam.

Table 6. Summary of determinations of polarity correction for chamber IBA FC65-G #1233

Measurement	Location	Electrometer	HT (V)	P_{pol}[1]	Relative std unc
In-water	NRC	Keithley 35617	-300	0.9995	0.0002
In-water	NRC	SI Supermax	-300	0.9996	0.0003
In-air	NRC	Keithley 35617	-300	0.9997	0.0002
In-air	LMRI	SI Supermax	-300	0.9995	0.0003

[1] Correction to reading collecting positive charge (HT negative)

The doserates of the two Co-60 beams are quite different (0.85 Gy min^{-1} at NRC, compared to 0.25 Gy min^{-1} at LMRI), due to the activity of the sources. Therefore, one must at least consider the impact of ion recombination on the comparison. The ion recombination correction can generally be split into two components– initial and general (e.g., Burns and McEwen, 1998). For therapy-level Co-60 beams and ionization chambers of the type used in this comparison operated with a polarizing voltage of 200 V to 300 V, general recombination can be ignored as it is generally less than 0.05 %. Initial recombination is measurable and typically of the order of 0.1 % to 0.2 %. However, since initial recombination is independent of the doserate it will cancel and therefore no correction for recombination is required.

3.6 Comparison of standards of air kerma

Each chamber was positioned in-air such that the front edge of the chamber thimble was at the 80 cm position as indicated by the light distance indicator. The mechanical pointer was used to verify this distance (within 0.5 mm) without touching the chamber. The chamber axis was perpendicular to the beam axis within 1 degree and the centre of the thimble was aligned with the centre of light field within 1 mm (resolution of light field cross-hairs). The build-up cap of the chamber was then fitted, ensuring that during this process there was no change in the chamber position. The various components are shown in Figure 8.

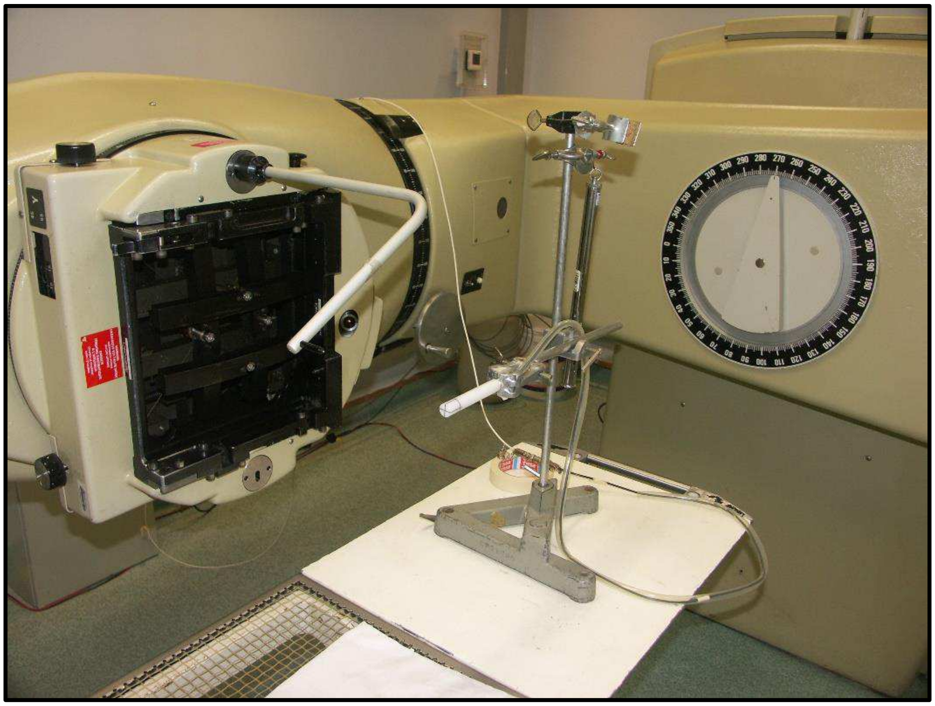

Figure 8. Setup for determination of air kerma rate.

The outer diameters of the two chambers are different, FC65-G = 7.1mm, NE2611 = 8.4 mm, so an inverse-square correction of 1.0016 was applied to the NE2611 chamber reading to correct for the difference in positions of the respective centres of the chambers. Due to the difficulty in the setup procedure only the FC65-G chamber was set up twice, to confirm repeatability. In each case there was at least a 10-minute pre-irradiation followed by five 60-second irradiations. Both chambers were connected to the same electrometer – the NRC Standard Imaging Supermax S/N P082341. For the IBA FC-65G the polarizing voltage was set to -300 V (collecting positive charge) and for the NE2611 the polarizing voltage was set to +200 V (collecting negative charge). These settings correspond to the calibration conditions at NRC and NPL respectively. The results are shown in Table 7.

Table 7. Summary of determinations of the air kerma rate

Chamber	Raw ion current (pA)	Standard deviation[1] (%)	P_{TP}[2]	Corrected ion current[3] (pA)	Air kerma rate (mGy min^{-1})
IBA FC65-G #1233	96.60	0.02	1.0820	104.53	280.3
IBA FC65-G #1233	-97.06	0.01	1.0755	-104.40	280.2[4]
NE2611 #1023	-45.36	0.02	1.0864	-49.29	278.7[5]

[1] This is the standard deviation for 5 repeat readings of 60 s each.
[2] The correction for air density is different for the two chambers because of the different reference temperatures at calibration (NRC = 22 °C, NPL = 20 °C).
[3] The leakage currents for the chambers during the measurements varied slightly in the range ± 9 fA, which is less than a 0.03 % contribution to the ion chamber signal. No correction for leakage was applied.
[4] The second measurement of the FC65-G was acquired at the opposite polarity and then the mean polarity correction from Table 6 was used to correct the ionization current.
[5] Includes inverse-square correction of 1.0016 to take account of difference in chamber SCDs (see text above table).

This gives a mean value for the ratio **K_{LMRI}/K_{NRC} = 0.9945**. The uncertainty in the ratio is discussed in section 3.8.

3.7 Comparison of standards of absorbed dose

Measurements were made in an IAEA calibration water phantom with a thin entrance window. The radiation field settings were SSD = 80 cm (using mechanical pointer, verified with light distance indicator) and field size = 10 cm x 10 cm. The phantom was placed on the beam axis with an uncertainty of 1 mm (resolution of light field indicator) and the phantom front window was perpendicular to the beam axis within 1 degree. The chambers were placed in PMMA sleeves (the NE2611 chamber is not waterproof) at a fixed depth of 10 cm, as shown in Figure 9.

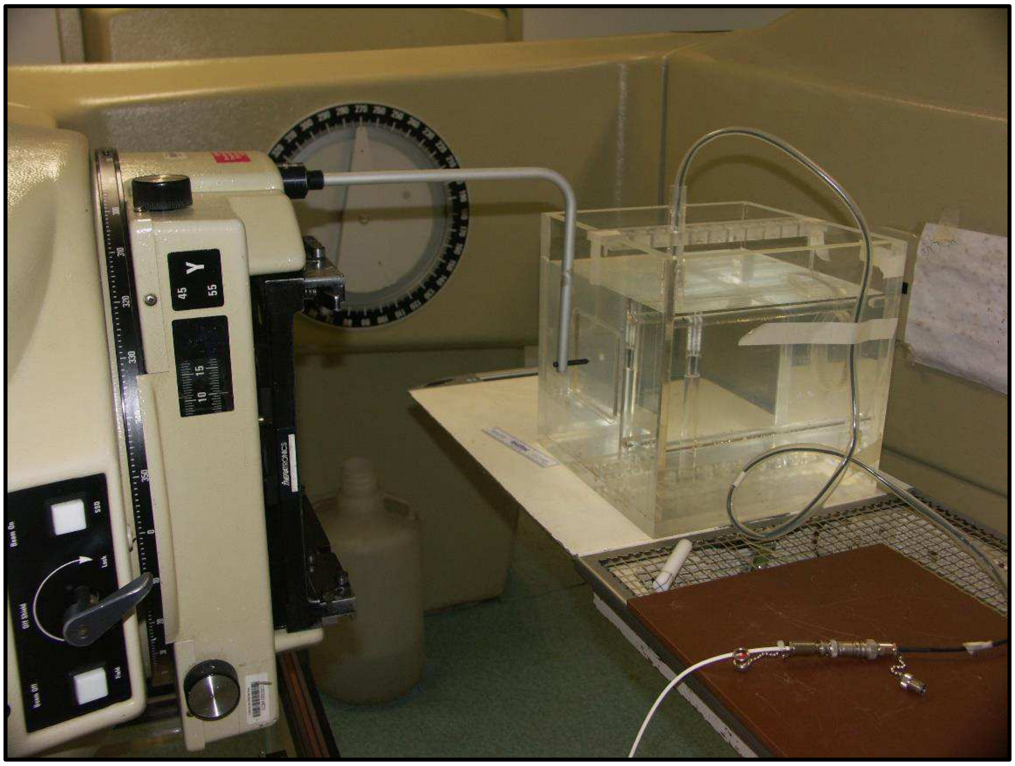

Figure 9. Setup for comparison in water

Each chamber was set up in the phantom twice and in each case there was at least a 10-minute pre-irradiation followed by five 60-second irradiations. Both chambers were connected to the same electrometer – the NRC Standard Imaging Supermax S/N P082341. For the IBA FC-65G the polarizing voltage was set to -300 V (collecting positive charge) and for the NE2611 the polarizing voltage was set to +200 V (collecting negative charge). These settings corresponded to the calibration conditions at NRC and NPL respectively. The results are shown in Table 8.

Table 8. Summary of determinations of the absorbed dose rate to water

Chamber	Raw ion current (pA)	Standard deviation[1] (%)	P_{TP}[2]	Corrected ion current[3] (pA)	Absorbed dose rate to water (mGy min^{-1})
IBA FC65-G #1233	57.07	0.02	1.0805	61.67	179.5
NE2611 #1023[4]	-26.88	0.07	1.0878	-29.25	178.7
IBA FC65-G #1233	57.00	0.03	1.0798	61.55	179.2
NE2611 #1023[4]	-26.93	0.03	1.0873	-29.29	179.0

[1] This is the standard deviation for 5 repeat readings of 60 s each.
[2] The correction for air density is different for the two chambers because of the different reference temperatures at calibration (NRC = 22 °C, NPL = 20 °C).
[3] The leakage currents for the chambers during the measurements varied slightly in the range ± 6 fA, which is less than a 0.02 % contribution to the ion chamber signal. No correction for leakage was applied.
[4] Measurements of the chamber positions in-phantom indicated that there was a small difference in the measurement depth between the two chambers (0.5 mm). A correction of 1.0034 was applied to the NE2611 readings (based on the measured depth-dose curve) to take account of this.

This gives a mean value for the ratio **D_{LMRI}/D_{NRC} = 0.9972.** The uncertainty in the ratio is discussed in section 3.8.

3.8 Uncertainties

The detailed uncertainty budgets for the air kerma and absorbed dose comparisons are given in Tables 9 and 10 respectively. Although there are different components of uncertainty in the two comparisons, the overall standard uncertainty in the ratio measurement for each quantity is very similar, approximately 0.9 %. For this comparison no correlations have been considered for the NRC and NPL primary standards. For air kerma the correlations are likely to be more significant, due to both standards being graphite-walled cavity chambers. For the absorbed dose measurement, the two primary standard calorimeters are very different (NRC – water, NPL – graphite) so there will be little or no correlation.

Table 9. Uncertainty budget for the comparison of air kerma standards

Component	Value	Unit	Relative standard uncertainty	
			$u_{i,A}$	$u_{i,B}$
NRC IBA FC65-G #1233				
Set up - SCD precision	0.25	mm		0.0006
Set up - repeatability				0.0001
Charge measurement			0.0002	
Chamber stability - day-to-day				0.0001
Chamber stability - longer term[1]				0.0010
Electrometer calibration				0.0003
T precision	0.1	°C		0.0003
T stability	0.05	°C		0.0002
P precision	0.1	mb		0.0001
P stability	0.1	mb		0.0001
			Combined	**0.0013**
CCHEN NE2611 #1023				
Set up - SCD precision	0.25	mm		0.0006
Set up - repeatability				
Charge measurement			0.0002	
Chamber stability - day-to-day				0.0003
Chamber stability - longer term[2]				0.0014
Electrometer calibration				0.0003
T precision	0.1	°C		0.0003
T stability	0.05	°C		0.0002
P precision	0.1	mb		0.0001
P stability	0.1	mb		0.0001
Inverse square correction				0.0003
			Combined	**0.0017**
Standard uncertainty in the determination of the charge ratio (combine the uncertainties for the two chambers)				**0.0021**
Uncertainty in NRC N_K calibration coefficient				**0.0050**
Uncertainty in NPL N_K calibration coefficient				**0.0065**
Uncertainty in C_K value (see text)				**0.0013**
Standard uncertainty in the kerma rate comparison NRC-LMRI				**0.0086**

[1] Derived from historical calibration data for this chamber
[2] Based on NPL data for chambers of the same type
[3] Required because reference position is front outer surface of ion chamber and NE2611 has different diameter to FC65-G

Table 10. Uncertainty budget for the comparison of absorbed dose to water standards

Component	Value	Unit	Relative standard uncertainty $u_{i,A}$	$u_{i,B}$
NRC IBA FC65-G #1233				
Set up - SSD precision[1]	0	mm		0.0000
Set up - depth setting	0.25	mm		0.0017
Set up - repeatability				0.0013
Charge measurement			0.0002	
Chamber stability - day-to-day[2]				0.0001
Chamber stability - longer term				0.0004
Electrometer calibration				0.0003
T precision	0.1	°C		0.0003
T stability	0.05	°C		0.0002
P precision	0.1	mb		0.0001
P stability	0.1	mb		0.0001
Field uniformity				0.0005
			Combined	**0.0023**
CCHEN NE2611 #1023				
Set up - SSD precision	0	mm		0.0000
Set up - depth setting	0.25	mm		0.0017
Set up - repeatability				0.0010
Charge measurement			0.0002	
Chamber stability - day-to-day				0.0003
Chamber stability - longer term[3]				0.0014
Electrometer calibration				0.0003
T precision	0.1	°C		0.0003
T stability	0.05	°C		0.0002
P precision	0.1	mb		0.0001
P stability	0.1	mb		0.0001
Depth correction[4]				0.0007
Field uniformity				0.0005
			Combined	**0.0027**
Standard uncertainty in the determination of the charge ratio (combine the uncertainties for the two chambers)				**0.0035**
Uncertainty in NRC NK calibration coefficient				**0.0050**
Uncertainty in NPL NK calibration coefficient				**0.0065**
Standard uncertainty in the absorbed dose comparison NRC-LMRI				**0.0089**

[1] Same phantom used for both chambers
[2] Derived from comparison of calibrations at NRC before and after LMRI measurements
[3] Based on NPL data for chambers of the same type
[4] Chamber holders for the two types positioned the chamber at a slightly different depth in-phantom (see earlier text).

4 Discussion of results and effect of influence quantities

4.1 Dependence on electrometer

The primary electrometer used for the comparison was the NRC Standard Imaging Supermax S/N P082341. This instrument was cross-calibrated against the reference electrometer used at the NRC Co-60 facility, a Keithley 35617, as shown in Table 2. During the measurements at LMRI, the two comparison chambers were connected to a number of other electrometers – Keithley 6517B S/N 4101709, NE2560 S/N 227 and NE2670 S/N 227. The NE2560 could only be used with a NE2561 chamber (see section 4.3) and the NE2670 showed problems with a high leakage current and measurement instabilities. The performance of the Keithley 6517B is shown in Table 11, compared to the SI Supermax. There is very good agreement between the readings for the two electrometers (a mean difference of 0.06 % with a standard uncertainty of 0.03 %). There is no dependence on the chamber connected and no difference in the standard deviation for a set of five 1-minute irradiations. The charge accuracy of the 6517B is consistent with the experience at the NRC with Keithley 6517A electrometers.

Table 11. Comparison of electrometer performance

Chamber	SI Supermax		Keithley 6517B		
	Reading (pA)	Standard deviation[1] (%)	Reading (pA)	Standard deviation (%)	R_{6517B} / $R_{Supermax}$
IBA FC65-G	104.40	0.01	104.36	0.02	0.9996
NE2611	49.29	0.02	49.25	0.03	0.9992
NE2611	29.29	0.03	29.27	0.01	0.9993

[1] This is the standard deviation for 5 repeat readings of 60 s each.

4.2 Dependence on phantom type and beam orientation

For the absorbed-dose component, measurements were made with three different phantoms during the course of the comparison:

1) IAEA calibration water phantom, horizontal beam, thin PMMA entrance window
2) NE PMMA intercomparison phantom
3) CNMC 1-D calibration water phantom, vertical beam, no entrance window

Only the first two could be used for comparison of the NRC and LMRI standards as there was no waterproofing sleeve available that would allow the positioning of the LMRI NE2611 chamber in the CNMC phantom. However, doserate determinations using the NRC waterproof chamber were acquired in all three phantoms for the same SSD and field-size settings, and these are shown in Table 12.

Table 12. Summary of determinations of doserate using different phantoms for the same ionization chamber, SSD and field-size settings

Phantom	Material	Beam orientation	Date	Doserate (mGy/min)	Doserate ratio *(relative to first setup)*
IAEA	water	Horizontal	6-Oct-16	179.5	1.000
IAEA	water	Horizontal	7-Oct-16	179.2	0.998
NE	PMMA[1]	Horizontal	11-Oct-16	179.9	1.002
CNMC	water	Vertical	11-Oct-16	178.9	0.997
CNMC	water	Vertical	11-Oct-16	179.9	1.002

[1] The chamber reading in the PMMA phantom was acquired at a depth of 10 cm in PMMA. This was then corrected to 10 cm water equivalent depth using the depth-dose data shown above (Figure 6) and assuming a relative electron density of 1.15.

There are both inter-phantom and intra-phantom variations in the measured doserate, but the overall standard deviation is only 0.25 %, indicating no significant dependence on either phantom or beam direction. The PMMA phantom is of interest because it is simpler to use for regular QA measurements than either water phantom. A comparison of the NRC and LMRI standards was therefore carried out in PMMA, using the standard inserts for the two chamber types. The result of this comparison is shown in Table 13.

Table 13. Summary of determinations of the absorbed dose rate to water **in PMMA**

Chamber	Raw ion current (pA)	Standard deviation[1] (%)	P_{TP}[2]	Corrected ion current[3] (pA)	Absorbed dose rate to water (mGy min^{-1})
IBA FC65-G #1233	53.12	0.01	1.0825	57.50	167.4
NE2611 #1023	-25.11	0.03	1.0896	-27.36	166.6

[1] This is the standard deviation for 5 repeat readings of 60 s each.
[2] The correction for air density is different for the two chambers because of the different reference temperatures at calibration (NRC = 22 °C, NPL = 20 °C).
[3] The leakage currents for the chambers during the measurements varied slightly in the range ± 7 fA, which is less than a 0.03 % contribution to the ion chamber signal. No correction for leakage was applied.

This gives a value for the dose ratio, $D_{LMRI}/D_{NRC} = 0.9953$, which is within 0.2 % of the in-water measurement. Although this measurement does not provide a direct comparison of the two labs' disseminations of absorbed dose to water, it serves to confirm the dose ratio obtained in the water phantom, specifically indicating that there were no significant errors related to the setup for that comparison. Despite the simpler setup for the PMMA phantom, water should remain the reference material for absolute dose measurement and calibration, as recommended in international dosimetry protocols such as IAEA TRS-398 and AAPM TG-51 (IAEA, 2000; Almond *et al*, 1999; McEwen *et al*, 2014).

4.3 Level of agreement between NRC and LMRI standards

As can been from Tables 7 to 10, the NRC and LMRI standards agree within the stated uncertainties. This validates the traceability of the LMRI to the NPL primary standards. One can use the data in the BIPM Key Comparison Database (http://kcdb.bipm.org) to check the consistency of the comparison ratios obtained here. Ignoring any variations due to chamber stability, experimental set up, *etc*, one would expect that the LMRI/NRC ratios would be equal to the NPL/NRC ratios published in the KCDB. The comparison of these two ratios is shown in Table 14.

Table 14. Comparison of results with KCDB

	Absorbed dose to water	Air kerma
LMRI/NRC	0.9972	0.9945
NPL/NRC	1.0000	0.9979

The differences in these ratios are 0.28 % and 0.34 % for absorbed dose and air kerma respectively. These differences are consistent with the standard uncertainties in Tables 9 and 10, if the components for the primary standards are removed (since these are correlated in the comparison in Table 14). There is therefore no discrepancy between the comparison carried out at the LMRI and internationally-recognized degrees of equivalence.

4.4 Verification of the results of this comparison

It should be noted that this is an informal, bi-lateral comparison. The procedure was very similar to what would occur in a formal comparison but the measurement protocol was not agreed in advance and the comparison was not formally registered through a recognized body such as SIM (Sistema Interamericano de Metrologia) or the CIPM (Comité international des poids et mesures) consultative committee on ionizing radiation, CCRI(I). The comparison, however, can be used to support CMC declarations and as part of a Quality System accreditation/recognition process.

It is worth discussing how this comparison can be validated, or the standards dissemination of LMRI-CCHEN be more formally recognized. In the short-term, an obvious step would be for LMRI-CCHEN to participate in a SIM-sponsored CCRI(I) supplementary comparison. The last such comparison was reported in 2008, so a repeat on the standard 10-year cycle is due.

The choice of traceability is also something to consider. Maintaining traceability to the NPL provides a stable metrological basis for air kerma and absorbed dose dissemination in Chile, but LMRI-CCHEN could choose to develop its own primary standards. For air kerma it is a case of constructing a cavity standard ionization chamber (or purchasing such an item, as a number of NMIs and DIs have done). For absorbed dose to water, there are a wider range of techniques, as indicated in the IAEA TRS-398 code of practice. Fricke dosimetry is a technique already available to LMRI-CCHEN and would therefore seem an appropriate option. Whether the Fricke dosimeter is a primary or secondary system depends on one's perspective of the G-value. There is evidence (McEwen and Ross, 2009) to suggest that for standard Fricke solutions (i.e., using a recommended recipe) the G-value is independent of the individual situation and can be viewed as a conversion constant (in a way equivalent to W_{air} in air kerma standards). In well-controlled situations (Klassen *et al*, 1999), Fricke dosimetry has been shown to yield uncertainties similar to other primary devices such as water or graphite calorimeters.

5. Conclusion

The Co-60 unit installed at the LMRI-CCHEN laboratory has been successfully commissioned and a comparison of NRC and LMRI standards for absorbed dose to water and air kerma in Co-60 has been completed. The results agree within the experimental uncertainties and are consistent with data in the CIPM KCDB.

References

P. Almond, P. J. Biggs, B. M. Coursey, W. F. Hanson, M. S. Huq, R. Nath, and D.W.O. Rogers, "AAPM's TG-51 protocol for clinical reference dosimetry of high-energy photon and electron beams", *Med Phys.* **26**:1847 (1999)

D. T. Burns and M. R. McEwen, "Ion recombination corrections for the NACP parallel-plate chamber in a pulsed electron beam", *Phys. Med. Biol.* **43** p2033-2045 (1998)

I. J. Das, C-W Cheng, R. J. Watts, A. Ahnesjö, J. Gibbons, X. A. Li, J. Lowenstein, R. K. Mitra, W. E. Simon and T. C. Zhu, "Accelerator beam data commissioning equipment and procedures: Report of the TG-106 of the Therapy Physics Committee of the AAPM," *Med. Phys.* **35** 4186-4215 (2008)

IAEA (International Atomic Energy Agency) *Absorbed Dose Determination in External Beam Radiotherapy (IAEA Technical Reports Series No. 398)* (Vienna: IAEA) (2000)

N.V. Klassen, K. R. Shortt, J. Seuntjens, and C. K. Ross, "Fricke dosimetry: The difference between G(Fe3+) for ^{60}Co g-rays and high-energy x-rays." *Phys. Med. Biol.* **44**:1609–1624 (1999)

J. P. McCaffrey, B. Downton, H. Shen, D. Niven and M. R. McEwen, "Pre-irradiation effects on ionization chambers used in radiation therapy" *Phys. Med. Biol.* **50** N121-N133 (2005)

M. R. McEwen and C. K. Ross, "Fricke and Alanine Dosimeters" in "Clinical Dosimetry Measurements in Radiotherapy" eds D Rogers and J Cygler, Medical Physics Publishing, Wisconsin (2009)

M. R. McEwen, "Measurement of ionization chamber absorbed dose k_Q factors in megavoltage photon beams," *Med. Phys.* **37** 2179-2193 (2010)

M. McEwen, L. DeWerd, G Ibbott, D. Followill ,D. W. O. Rogers, S. Seltzer, J. Seuntjens, "Addendum to the AAPM's TG-51 Protocol for Clinical Reference Dosimetry of High-Energy Photon Beams" *Med. Phys.* **41**, 041501 (2014)

Nutbrown, R, private communication (2013)

J. D. Ververs, M. J. Schaefer, I Kawrakow and J. V. Siebers, "A method to improve accuracy and precision of water surface identification for photon depth dose measurements," *Med. Phys.* **36** 1410-1420 (2009)